Mouse oocytes do not contain a conventional Balbiani body

Laasya Dhandapani[1], Marion Salzer[1], Juan M. Duran[1], Gabriele Zaffagnini[1], Cristian De Guirior[2], Maria Angeles Martínez-Zamora[2], Elvan Böke[1,3*]

[1]Centre for Genomic Regulation (CRG), The Barcelona Institute of Science and Technology, Dr. Aiguader 88, Barcelona 08003, Spain;
[2] Instituto Clínic de Ginecología, Obstetricia y Neonatología (ICGON), Hospital Clínic, Barcelona, Spain;
[3]Universitat Pompeu Fabra (UPF), Barcelona, Spain
* Corresponding Author

Correspondence to Elvan Böke: elvan.boke@crg.eu
ORCID ID: 0000-0002-0760-7353
Mailing Address: Centre for Genomic Regulation (CRG), Dr. Aiguader 88, Edifici PRBB Barcelona 08003, Spain

ABSTRACT

Poor oocyte quality accounts for majority of female fertility problems, however, we know little about how oocytes can remain healthy for many years or why they eventually decline with age. An oocyte spends majority of its lifetime in primordial state. Unlike many somatic cell types or mature oocytes, the cellular and molecular biology of primordial oocytes are largely unexplored. Yet, studying these aspects is necessary to understand the remarkable lifespan of oocytes and their eventual decline.

A hallmark of primordial oocytes in many species is the Balbiani body, a non-membrane bound compartment that contains majority of mitochondria in oocyte cytoplasm. The Balbiani body was shown to be held together by an amyloid-like matrix in *Xenopus* oocytes. It has been proposed to be essential for maintaining mitochondria in a healthy state during long-lasting dormancy.

Here, we develop enabling methods that allow live-imaging based comparative characterisation of *Xenopus*, mouse and human primordial oocytes. We show that human and *Xenopus* oocytes have a Balbiani body, characterised by an intense accumulation of mitochondria. Our results suggest that amyloid-like features of Balbiani bodies are conserved in humans and *Xenopus*. However, despite previous reports, we could not find a conventional Balbiani body in mouse oocytes. We demonstrate what was mistaken for a Balbiani body in mouse primordials is an unconventionally shaped Golgi apparatus. Our work provides the first insights into the organisation of the cytoplasm in mammalian primordial oocytes, and clarifies relative advantages and limitations of different model systems for studying female (in)fertility.

Significance Statement

World-wide data suggest that >25% of female fertility problems are undiagnosed, pointing to a huge gap in our understanding of female reproduction. Our findings help fill this gap by studying the cell biology of primordial oocytes. Having optimised methods for isolation and live-imaging of oocytes, we show that oocytes of evolutionary more distant species, Xenopus and human have a conserved super-organelle, a Balbiani body, in their cytoplasm whereas mouse oocytes do not have one. We propose that the shorter lifespan in mice obviates the need for a Balbiani body. Our results also suggest that primordial oocytes have active organelles, and thus call for a re-examination of the concept of dormancy in these long-lived cells.

INTRODUCTION

Oocytes, female germ cells that become eggs, are considered very long-lived. They can remain in the ovary for long periods of time, ranging from several weeks in mice to several decades in humans (Flurkey et al., 2007; Wallace and Kelsey, 2010). In mammals, the number of oocytes is fixed at the neonatal stage, which represents the entire population of available oocytes throughout the female reproductive lifespan. The earliest stage of recognizable oocytes in an ovary, which also constitute the ovarian reserve, is called primordial oocytes. Primordial oocytes are considered dormant, as they do not grow nor divide (Reddy et al., 2010). From the pool of thousands of primordial oocytes, only a few are activated to grow at any given time. Upon sexual maturity, some of the growing oocytes mature to produce fertilizable oocytes, called eggs (Grive and Freiman, 2015; Rimon-Dahari et al., 2016).

The major morphological feature of primordial oocytes of many species is a cytoplasmic conglomeration of organelles, called the Balbiani body. The Balbiani body is a non-membrane bound super-organelle consisting mostly of mitochondria but also Golgi complexes, endoplasmic reticulum (ER), other vesicles and RNA (Boke et al., 2016; Cox and Spradling, 2003; Hertig, 1968; Kloc et al., 2004). The Balbiani body is held together by an amyloid-like matrix formed by an intrinsically disordered protein in frogs and in zebrafish (Boke et al., 2016; Krishnakumar et al., 2018). The Balbiani body is only present in early, non-growing oocytes and dissociates upon oocyte activation, thus is closely associated with oocyte dormancy. The function of the Balbiani body remains elusive, although it is proposed to protect mitochondria and RNA in the germline (Jamieson-Lucy and Mullins, 2019; Kloc et al., 2004). This enigmatic super-organelle has been observed in, among others, humans (Hertig and Adams, 1967), monkeys (Hope, 1965), cats (Amselgruber, 1983), frogs (Al-Mukhtar and Webb, 1971; Boke et al., 2016) and zebrafish (Marlow and Mullins, 2008). Recent research suggested that mouse primordial oocytes also contain a Balbiani body (Lei and Spradling, 2016; Pepling et al., 2007).

Since oocytes contribute virtually all of the organelles and cytoplasm to the zygote and hence, the new embryo, maintenance of oocyte health is imperative for producing healthy offspring. Although there is growing knowledge on how

oocytes grow and interact with their somatic environment(Handel et al., 2014; Matzuk et al., 2002), and how they segregate their chromosomes (Holubcová et al., 2015; Pfender et al., 2015), research on dormant oocytes, in which an oocyte spends majority of its life, is virtually absent. To shed light on the paradoxical youth of babies born from old oocytes, we characterised and compared cytoplasmic features of frog, mouse and human primordial oocytes, which are complementary for their ease of handling and relevance to human physiology.

RESULTS

Cytoplasmic organization of organelles is similar in *Xenopus* and human oocytes, but different in mouse

Live characterisation of cells can reveal features that are lost after fixation such as organelle dynamics and activity. We began our studies by isolating oocytes from mouse, human, and frog ovaries (Figure 1A) for live imaging. *Xenopus laevis* (frog) and human oocytes were isolated after collagenase treatment, and left within their follicles, because somatic cells surrounding the oocyte, called granulosa cells, serve as excellent internal controls to compare somatic cells to oocytes (Figure 1A-D). Mouse primordial oocytes had to be isolated via trypsin treatment of ovaries due to their low collagen content, which led to the detachment of pre-granulosa cells (Figure 1A). Thus, they were imaged without granulosa cells.

Xenopus laevis early stage oocytes were large (approximately 200 μm in diameter) and exhibited a discernible Balbiani body next to their nucleus (Figure 1A). The granulosa cells were only visible when stained with fluorescent markers in maximum z-projections (Figure 1B-D). Primordial oocytes in humans were approximately 30 μm in diameter and displayed a crescent-shaped Balbiani body adjacent to their nucleus (Figure 1A-D). In all human primordial oocytes imaged, there was a central mass roughly in the middle of the Balbiani body which was also observed in electron microscopy images (Baca and Zamboni, 1967; Hertig, 1968; Hertig and Adams, 1967) (Figure 1A,B). The molecular composition of this mass is not known. Primordial oocytes in mice were 15-17 μm in diameter. Due

to their small size, their cytoplasmic features are hard to appreciate with transmitted light microscopy (Figure 1A).

We probed oocytes with fluorescent markers for mitochondria, lysosomes and Golgi apparatus to investigate the distribution of organelles in oocyte cytoplasm. We imaged mitochondria in oocytes using tetramethylrhodamine ethyl ester (TMRE), a cell-permeant fluorescent dye that accumulates in active mitochondria dependent on mitochondrial membrane potential (Ehrenberg et al., 1988). All three vertebrate oocytes had detectable mitochondrial membrane potential as judged by TMRE staining (Figure 1B). Treatment of oocytes with CCCP, an ionophore, to dissipate the membrane potential (Heytler, 1963) led to the loss of TMRE staining, confirming its specificity (Figure S1A). In human and *Xenopus* oocytes, majority of the mitochondria were present within the Balbiani body as observed in the literature (Boke et al., 2016; Hertig and Adams, 1967) (Figure 1B). However, mitochondria of mouse oocytes were distributed throughout the cytoplasm (Figure 1B, Figure S1C), showing a different cytoplasmic pattern than oocytes of the other two species; human and *Xenopus*.

Next, we used Lysotracker Deep Red to image lysosomes. Lysotracker is a membrane-permeable dye that preferentially accumulates in acidic lysosomes, and thus, is used to assess the activity status of lysosomes (Zhang, 1994). Lysosomes in primordial oocytes of all three vertebrate species stained with Lysotracker (Figure 1C). This staining was lost upon incubation of oocytes with bafilomycin A1, which prevents lysosomal acidification via inhibition of the V-ATPase activity (Bowman et al., 1988), confirming specificity of Lysotracker dye (Figure S1B). The lysotracker intensity was similar between pregranulosa cells and primordial oocytes in human and Xenopus (Figure 1C) as well as between primordial oocytes and growing oocytes (GVs) in mouse (Figure S1C). Thus, we concluded that primordial oocytes have acidic lysosomes distributed in their cytoplasm.

We used a fluorescent derivative of ceramide, NBD-C_6 Ceramide to image the Golgi Apparatus in live oocytes. NBD-C_6 Ceramide is taken up by cells and transported to the Golgi apparatus, where it is metabolized and localized to the

late Golgi cisternae (Lipsky and Pagano, 1985; Pagano et al., 1989). *Xenopus* and human oocytes displayed a distributed pattern of Golgi in their cytoplasm, whereas in mouse oocytes, NBD-C_6 Ceramide showed a specific staining previously described as a Golgi conglomerate (Figure 1D, S1D, Movie S1) (Wischnitzer, 1970). The Golgi conglomerate in mouse oocytes, or the moniker, a Golgi ring from here on, was not present in growing oocytes (Figure S1E, 2A).

Live-characterisation of primordial oocytes of three vertebrates revealed that mouse primordial oocytes are different from human and *Xenopus* oocytes such that they do not have any mitochondrial conglomeration and have an unconventionally shaped Golgi apparatus (the Golgi ring) in their cytoplasm.

The Golgi ring in mouse primordial oocytes have features of a conventional Golgi apparatus

The Golgi ring was previously referred as the Balbiani body in mouse oocytes (Lei and Spradling, 2016; Pepling et al., 2007) and is the most prominent cytoplasmic feature in these cells, different from human and *Xenopus* oocytes. We therefore asked whether the Golgi ring displayed features of a canonical Golgi apparatus.

First, we checked whether it contained conventional polarized Golgi stacks, containing both *cis*- and *trans*- cisternae. For that, immunostaining was performed on ovary sections with a cis-Golgi marker, GM130, and a trans-Golgi marker, TGN46. The Golgi ring contains both markers (Figure 2A), which were tightly apposed with the cis-compartment facing outwards and the trans-compartment inwards (Figure 2A, C). This suggests that the Golgi ring has structural features of a conventional Golgi apparatus.

In most vertebrate cells, the Golgi apparatus localizes near the nucleus and surrounds the centrosome (Sütterlin and Colanzi, 2010). Therefore, we asked whether the Golgi ring associates with pericentrin, a centrosome marker (Doxsey et al., 1994), in primordial oocytes. Indeed the Golgi membranes visualized with TGN46 accumulated around pericentrin (Figure 2B,C). Taken together, these data suggest that the Golgi ring is comprised of stacks arranged around the centrosome, as expected from a conventional Golgi apparatus.

Finally, we asked whether the Golgi ring is capable of membrane trafficking to investigate its function. Brefeldin A (BFA) is a fungal metabolite that induces extensive tubulation of Golgi apparatus cisternae and its ultimate fusion to ER membranes. Hence, an active Golgi apparatus should be quickly taken apart by BFA action (Lippincott-Schwartz et al., 1990). Primordial oocytes were treated with Brefeldin A, followed by labelling the Golgi apparatus with NBD-C_6 Ceramide and live cell imaging. The Golgi ring was present in nearly 60% of untreated oocytes (Figure 3A, B). Brefeldin A treatment led to the dissociation of the Golgi ring (Figure 3A, B). We repeated our experiments in an outbred mouse strain, CD1, and obtained similar results. 80% of untreated oocytes had the Golgi ring, whereas only 20% had the Golgi ring in the Brefeldin A treated sample, suggesting that primordial oocytes in CD1 strain also disassembled their Golgi ring upon BFA treatment (Figure S2A, B). We thus conclude that the Golgi ring in mouse oocytes is capable of membrane trafficking and its structure is actively maintained.

We conclude that the Golgi ring displays properties of a conventional Golgi apparatus, structurally and functionally. The Golgi ring is also not a specific feature of germ cells: a similarly shaped Golgi apparatus in a juxtanuclear location was also described in rat pituitary gonadotrophs (Koga and Ushiki, 2006; Watanabe et al., 2012).

Having identified the most apparent structures in mouse primordial oocytes as Golgi rings, we set out to determine whether mouse primordial oocytes might nevertheless possess a feature of primordial oocytes in humans and many other vertebrates: A Balbiani body.

The Golgi ring is not a Balbiani body

A characteristic feature of the Balbiani body is the presence of mitochondria (Bilinski et al., 2017). Previous research used the Golgi ring as a marker for the Balbiani body in mouse primordial oocytes (Lei and Spradling, 2016; Pepling et al., 2007). Thus, we assessed whether the Golgi ring is associated with mitochondria. Live imaging of mitochondria and the Golgi ring together showed

that they were spatially segregated in the cytoplasm of mouse oocytes (Figure 3C, upper panel, Movie S2). In fact, a Mitochondrial Exclusion Zone (MEZ) was present around the Golgi ring (Figure 3C, arrow heads).

It could be possible that mouse primordial oocytes might be unique in possessing a Balbiani-like compartment that lacks mitochondria, but is comprised of the Golgi ring and RNA binding proteins held together by a protein matrix. Upon Golgi ring dissociation by Brefeldin A treatment, this hypothetical compartment would still occupy a space and would not allow the movement of large organelles such as mitochondria through. Thus, the MEZ should be maintained. To test this hypothesis, we performed live cell imaging of untreated and Brefeldin A treated mouse primordial oocytes labelled with Mitotracker Deep Red and NBD-C_6 ceramide to stain mitochondria and the Golgi, respectively. In untreated cells, in which the MEZ is intact, mitochondria occupied 19% of the cytoplasm (Figure 3C, D, and Figure S3). The MEZ disappeared and mitochondria redistributed throughout the entire cytoplasm upon Brefeldin A treatment, almost doubling mitochondrial occupancy to 35% of the cytoplasm (Figure 3C, D). This redistribution of mitochondria within the cytoplasm suggests that mouse oocytes lack a proteinaceous matrix holding components of a presumed Balbiani body.

Because the periphery of the Golgi ring lacks both mitochondrial congregation and a proteinaceous matrix, we conclude that mouse primordial oocytes lack a Balbiani body.

The Golgi ring disassembly follows oocyte activation

Lacking a Balbiani body, we next asked whether the Golgi ring is associated with dormancy in mouse primordial oocytes. To dissect the relationship between the Golgi ring and dormancy, we asked whether the Golgi ring disassembly could trigger oocyte activation.

The localization of the transcription factor FOXO3a serves as a dormancy marker in oocytes; it is nuclear in dormant oocytes, and is exported to the cytoplasm upon oocyte activation (Castrillon et al., 2003; Shimamoto et al., 2019). *In vitro* ovary cultures were performed to monitor the relationship between the Golgi ring

and FOXO3a in dormant and activated oocytes. All three biological replicates were performed with neonatal ovaries (P3) of female litter from the same birth to reduce variation between conditions. Ovaries were fixed at time 0 (after extraction), and after 1 and 5 hours of *in vitro* ovary culture and were processed for whole-mount imaging with GM130 and FOXO3a antibodies to check the presence of the Golgi ring, and the dormancy status of oocytes, respectively. As expected, at t=0, primordial oocytes had a nuclear FOXO3a staining and a Golgi ring, whereas growing primary oocytes had FOXO3a already exported to their cytoplasm, and a dissociating Golgi ring (Figure 4A). FOXO3a was nuclear in 67 to 100 % of all oocytes in neonatal (P3) ovaries, reflecting the primordial oocyte pool (Figure 4A, 4D). After 1 hour of *in vitro* tissue culture, oocytes started activating *en masse* as previously reported (Hayashi et al., 2020; Shimamoto et al., 2019). In two of the replicates, only a very small proportion of oocytes were left with nuclear FOXO3a signal, whereas a third biological replicate displayed slower FOXO3a export to the cytoplasm (Figure 4B-D). After 5 hours of *in vitro* culture, nuclear FOXO3a localization further decreased in all three replicates (Figure 4B-D). The Golgi ring was present in the oocytes irrespective of FOXO3a localization; >75% of oocytes still had the Golgi ring after 1 or 5 hours of *in vitro* culture (Figure 4B-E). This suggests that oocyte activation, and corresponding export of FOXO3a to the cytoplasm precedes the Golgi ring disassembly.

We next asked whether artificial disassembly of the Golgi ring would have any impact on oocyte activation. Golgi ring disassembly was induced by treating whole ovaries with Brefeldin A. One hour after Brefeldin A treatment, all oocytes disassembled their Golgi ring (Figure 4B, 4E, Movie S3-4). The percentage of oocytes with nuclear FOXO3a was comparable to untreated ovaries at the same time point for all three replicates (Figure 4D). This suggests that artificial disassembly of the Golgi ring does not induce oocyte activation.

Finally, ovaries were washed to remove Brefeldin A and cultured in Brefeldin A free medium for an additional 4 hours. Surprisingly, almost all oocytes reformed their Golgi ring (Figure 4B, 4E, Movie S5-6) although many already had exited dormancy, judged by their cytoplasmic FOXO3a staining at t=1 and 5 hours (Figure 4B, 4D). Thus, we conclude that the Golgi ring formation is reversible, and not linked to the dormancy status of the oocyte.

Taken together, we conclude that the Golgi ring disassembly follows oocyte activation in vivo, and does not have a causal function. Moreover, the fact that activated oocytes can have Golgi rings calls for caution to use the Golgi ring as a dormancy marker.

The amyloid-like features of the Balbiani body is conserved in human and *Xenopus* oocytes

The Balbiani body was shown to be held together by an amyloid-like matrix in *Xenopus* oocytes (Boke et al., 2016). A electron microscopy study on human oocytes also suggested that the Balbiani body contains electron opaque deposits embedded within a matrix of fine fibrils (Hertig, 1968). This prompted us to examine human and mouse oocytes for amyloid-like assemblies. Human and mouse ovary sections were probed with an aggresome dye, Proteostat. Proteostat stains cross beta-sheet rich structures in cells, that are considered the hallmark of amyloids (Nelson et al., 2005) and is widely used in the literature to stain amyloid-like proteins (Olzscha et al., 2017; Tao et al., 2020; Usmani et al., 2014). An antibody against a ubiquitous mitochondrial protein, citrate synthase, was used to mark mitochondria, and thus, the Balbiani bodies in human and *Xenopus* oocytes. Proteostat marked the Balbiani bodies of both *Xenopus* and human oocytes, whereas no specific structure was observed in mouse oocytes (Figure 5A, S4A). We conclude that the amyloid-like features of Balbiani bodies are conserved in humans and *Xenopus*. Moreover, the diffuse proteostat staining in mouse oocytes further supports our results that mouse oocytes do not have a Balbiani body.

DISCUSSION

Here we perform the first live analysis of primordial oocytes in three vertebrate species, *Xenopus*, mouse and humans, which revealed that mouse oocytes do not have a Balbiani body, but contain a modified Golgi apparatus in their cytoplasm. Our results highlight the importance of live-analyses for characterization of not well-known cell types or compartments: Previous reports from fixed or sectioned mouse ovaries had referred to a modified Golgi apparatus for a Balbiani body, due to a combination of the unusual cytoplasmic organization

of oocytes and a lack of organelle dynamics. Primordial oocytes have a spherical shape with a large nucleus, which does not leave enough space for other organelles to be equally distributed in the cytoplasm. These features exacerbated the deformations caused by thin sections or 2D imaging of fixed tissues in previous reports (Lei and Spradling, 2016; Pepling et al., 2007). A recent preprint also suggested that the Golgi ring might store mRNAs due to its presumed association with two RNA binding proteins, RNGTT (mRNA Capping Enzyme) and DCP1A (Lei et al., 2020). Controversially, same authors also showed the Golgi ring does not have any detectable RNA using a pan-RNA probe (Lei et al., 2020). RNGTT is a nuclear mRNA capping enzyme that interacts with RNA Polymerase II (Galloway and Cowling, 2019). We checked whether RNGTT indeed localizes to the Golgi ring, however, immunostaining of mouse ovary sections for RNGTT revealed only nuclear localization of the protein, as expected (Figure S5A,B). On the other hand, DCP1A is an mRNA decapping enzyme, and a P-body component (Swetloff et al., 2009), which also localises to the Golgi apparatus and E.R membranes (Huch et al., 2016). The structure observed by Lei Lei et al could in fact be DCP1A localised either to the Golgi Apparatus or to the P-bodies close to the E.R exit sites (Kilchert et al., 2010; Wilhelm et al., 2005).

We found that the Golgi ring in primordial oocytes is active in membrane trafficking and displayed conventional Golgi features despite its modified shape. This modified shape of Golgi apparatus is also reported in rat pituitary gonadotrophs (Watanabe et al., 2012). Although textbook images of the Golgi apparatus is typically displayed as crescent-shaped ribbon of cisternal stacks, oriented to the leading edge in migrating cells (Bisel et al., 2008), several different shapes of Golgi apparatus are reported in different cell types (Kreft et al., 2010; Lu et al., 2001; Rao et al., 2018). Both primordial oocytes and pituitary gonadotrophs are apolar, non-migratory and secretory cells (Eppig, 2001; Watanabe et al., 2012). It could be that such cells have an atypical disposition of the Golgi apparatus caused by a lack of polarized secretory activity and a specialized organization of the cytoskeleton.

Oocytes are considered long-lived in all three vertebrate species we examined: Human oocytes have the longest lifespan among the three, and can live up to 55 years (Wallace and Kelsey, 2010). *Xenopus laevis* oocytes can stay several years without growth in ovaries (Callen et al., 1980; Keem et al., 1979), whereas mouse oocytes have the shortest lifespan with 8 to 14 months (Rugh, 1968). The fact that the offspring does not inherit the senescence status of their parents indicate that the oocyte cytoplasm remains damage-free at the time of fertilisation. Previous research in invertebrates suggested that oocytes might shut down the activity of their organelles to prevent ageing (Bohnert and Kenyon, 2017; Sieber et al., 2016). Our data in vertebrate oocytes suggest that primordial oocytes in vertebrates have metabolically active organelles, suggested by lysotracker and NBD Ceramide staining of all three vertebrate oocytes. This, together with previous evidence which shows primordial oocytes in mouse have transcriptional activity (Pan et al., 2005), and active mTOR (Guo et al., 2018), calls for an overhaul of thinking in mammalian germ cell field, which mostly assumes dormant oocytes wait for a signal during maturation to become metabolically active.

Our data strongly suggest that mouse oocytes do not contain a canonical Balbiani body, while human and frog oocytes have Balbiani bodies. This is surprising, as humans and frogs are evolutionary more distant to each other than mouse is to either species. Balbiani bodies are enigmatic super-organelles; their only known function is to host healthy mitochondria and protect RNAs from degradation to be passed on to the new embryo in the form of germ plasm (Jamieson-Lucy and Mullins, 2019; Kloc et al., 2004; Marlow, 2017). Species that use inductive processes to specify their germline, such as mammals or axolotls, still contain a Balbiani body, indicating a conserved function for this super-organelle. Here, we speculate that the Balbiani body serves to protect the quality of mitochondria and other organelles, and its necessity depends on the length of the reproductive lifespan of the species, especially in animals that donot contain germ plasm. Long-lived species have to keep their non-growing oocytes in their ovaries several years or decades, and thus it is possible to argue that they need a Balbiani body to protect their cytoplasm. Mouse oocytes can live relatively short 9 months, and they may not need a protective super-organelle to keep their

cytoplasm damage-free. It is noteworthy that *Xenopus* and human oocytes are also similar to each other and different than mouse in regard to their meiotic spindle assembly. *Xenopus* and human zygotes inherit a centriole from the sperm whereas mouse oocytes do not inherit a centriole (Avidor-Reiss and Fishman, 2019; Clift and Schuh, 2013).

FIGURE LEGENDS

Figure 1. Distribution of mitochondria, lysosomes and the Golgi apparatus in vertebrate primordial oocytes (A) Top panel: Intact ovaries. Bottom panel: Individual oocytes after the isolation procedure. Oocytes were isolated from *Xenopus* ovaries by Collagenase IA digestion; from human ovaries by Collagenase III digestion and from neonatal mouse ovaries by Trypsin digestion, as they contain little collagen. All primordial oocytes have a clearly discernible nucleus (n), while the Balbiani body (BB) is visible only in *Xenopus* and human oocytes. Cartoon representation of oocytes depicts nucleus (n) in blue and Balbiani body (BB) in magenta. Note the crescent shaped Balbiani body (BB) bordering the nucleus in human oocytes, while the Balbiani body in Xenopus is spherical next to the nucleus. The Golgi ring of mouse oocytes is depicted in green. **(B-D)** Live-cell imaging of oocytes incubated with **(B)** 500nM of Tetramethyl rhodamine (TMRE) for 30 minutes to image mitochondria, **(C)** 50nM LysoTracker Deep Red for 30 minutes to image lysosomes, and **(D)** 3μM NBD C_6-Ceramide for 30 minutes to image Golgi Apparatus. All top panels show the central plane of the oocyte. Middle panels are maximum z-projections of equatorial regions and bottom panels are DIC images of the same oocyte. The nuclear envelope and plasma membrane are marked with dashed lines. Insets in Xenopus images are 4X magnification of marked boxes. At least three biological replicates were performed for all conditions, and representative images are shown. Scale bars: 10μm**.**

Figure 2. Golgi ring of mouse primordial oocytes is composed of Golgi stacks and surrounds pericentrin. Immunostaining of frozen sections of neonatal ovaries using antibodies against **(A)** GM130 (green) and TGN46 (magenta), **(B)** Pericentrin (green) and TGN46 (magenta). A magnification of a primordial oocyte with the Golgi ring and a primary oocyte without it are shown in the right panel in (A). A magnification of a primordial oocyte was shown in the right panel in (B). The nuclei of oocytes and somatic cells are marked by DAPI (blue). Scale bars: 10μm. Note GM130 antibody also stains the basement membrane (Lei and Spradling, 2016). **(C)** Quantification of tissue sections shown in representative images in (A) and (B) to score the localisation of TGN46 and pericentrin to the Golgi ring. At least 30 primordial oocytes were counted per replicate; 3 biological replicates were performed. Error bars=mean±S.D.

Figure 3. The Golgi ring does not represent a conventional Balbiani body. (A) Live imaging of mouse primoridal oocytes untreated (DMSO) or treated with Brefeldin A (BFA) and incubated with NBD C_6-Ceramide to image the Golgi Apparatus **(B)** Quantification of oocytes containing a Golgi ring in untreated versus BFA treated oocytes from 3 biological replicates. p-value=0.00034 estimated by student's t-test. **(C)** Live imaging of mitochondria and the Golgi Apparatus in untreated or BFA treated primordial mouse oocytes. Oocytes were treated with NBD C_6-Ceramide and MitoTracker Deep Red FM to image the Golgi Apparatus and mitochondria, respectively. The mitochondrial exclusion zone (MEZ) is indicated by white arrow heads. **(D)** Quantification of the area of oocyte cytoplasm occupied by mitochondria in untreated and BFA treated oocytes. Two biological replicates from a total of 6 animals are shown, p-value<0.0001 estimated by student's t-test. Error bars=mean±S.D. Scale bars: 10μm.

Figure 4. The Golgi ring is present in activated oocytes. Whole-mount immunostaining of neonatal ovaries with FOXO3A (magenta) and GM130 (green) antibodies. **(A)** Representative images of primordial (top) and primary (bottom) oocytes in ovaries fixed immediately after extraction (t=0). **(B)** Representative images of untreated ovaries or ovaries after BFA treatment. After 1 hour BFA treatment, ovaries were cultured in BFA free medium for 4 hours to observe the Golgi ring reformation. **(C)** Representative images for nuclear or cytoplasmic FOXO3a localization in oocytes with the Golgi ring (Top and Top middle), and without the Golgi ring (Bottom middle and bottom panel). Nuclei were marked by DAPI. Maximum z projections of 3 x 1μm sections are shown. **(D-E)** Quantification of wholemount images for **(D)** nuclear FOXO3a at different *in vitro* culture time points (0, 1 and 5 hours) and **(E)** the presence of the Golgi ring at different *in vitro* culture time points (0, 1 and 5 hours).

Each biological replicate is represented by a different colour. Unfilled circles and squares were treated with BFA; unfilled squares were later incubated in fresh medium. Filled circles represent untreated ovaries. Statistical analysis of FOXO3a nuclear localization and the presence of the Golgi ring between all conditions revealed no relation between the two (Linear Fit; p value=0,87 and RSquare=0,002). Three biological replicates were performed. Scale bars:10μm.

Figure 5. Human and Xenopus Balbiani bodies share amyloid-like features
Immunostaining of young adult human and mouse paraffin embedded ovary sections and *Xenopus* oocytes using Proteostat (green) and an antibody against citrate synthase to mark mitochondria (magenta). Nuclei were marked with DAPI (blue) in mouse and human sections. DAPI staining of giant *Xenopus* nuclei are very weak and thus, we used DIC images to mark the nucleus of *Xenopus* oocytes. Representative images from three biological replicates were shown, see Figure S4 for more images and full sections. Scale bars: 10μm.

Supplementary Figure 1. Live-cell imaging reveals metabolically active organelles in primordial oocytes (A-B) Primordial oocytes were isolated from neonatal mice and treated with **(A)** 30 μM CCCP to dissipate mitochondrial membrane potential, followed by incubation with TMRE to image mitochondria. **(B)** 100nM Bafilomycin A1 to deacidify lysosomes, followed by incubation with LysoTracker to image lysosomes. **(C)** Mouse primordial and growing, germinal vesicle stage (GV) oocytes were imaged together after incubation with LysoTracker. Note unattached somatic cells in the frame. Although GVs have more lysosomes, the mean intensity staining of lysotracker per puncta were very similar between primordial and GV oocytes. **(D)** 3D reconstruction of the distribution of mitochondria and localization of the Golgi ring from the oocyte in Figure 1C. Nucleus is depicted in white. **(E)** Growing, germinal vesicle (GV), oocytes were imaged live after incubation with 3μM NBD C_6-Ceramide for 30 minutes. Inset shows 2X magnification of the dashed box. Scale bars: 10μm.

Supplementary Figure 2. The Golgi ring disassembly upon BFA treatment is not strain-specific (A) Primordial oocytes isolated from outbred CD1 mice were treated with 10μM Brefeldin A (BFA) for 1.5 hours, incubated with 3μM NBD C_6 -Ceramide and imaged live. Scale bars are 10μm. **(B)** Quantification of oocytes with and without Golgi ring from (A). Data from 4 animals are represented.

Supplementary Figure 3. Quantification of mitochondrial occupancy. Untreated (DMSO) or BFA treated primordial oocytes were incubated with 3μM NBD C_6-Ceramide and 100nM MitoTracker Deep Red FM for 30 minutes and imaged live. Oocyte periphery and nuclei were marked from DIC images, and the cytoplasmic area (i.e excluding nucleus) was calculated for each section. A mask was created to select mitochondria using the threshold function in Fiji/ ImageJ. Mitochondrial occupation of the cytoplasm was calculated by dividing the area occupied by mitochondria with the available cytoplasmic area.

Supplementary Figure 4. Human and Xenopus Balbiani bodies share amyloid-like features (A) Immunostaining of young adult human and mouse paraffin embedded ovary sections and *Xenopus* oocytes using Proteostat and an antibody against citrate synthase to mark mitochondria. Nuclei were marked with DAPI in mouse and human sections. DAPI staining of giant *Xenopus* nuclei are very weak and thus, we used DIC images to mark the nucleus of *Xenopus* oocytes. Scale bars are as indicated on the figure.

Supplementary Figure 5. RNGTT does not localize to the Golgi ring
(A) Immunostaining of frozen sections of neonatal ovaries using antibodies against GM130 (green) and RNGTT (magenta), The nuclei of oocytes and somatic cells are marked by DAPI (blue). Scale bars: 10μm. (B) At least 30 primordial oocytes were counted per replicate; 3 biological replicates were performed. All oocytes displayed nuclear RNGTT.

Movie S 1. The Golgi conglomerate, aka the Golgi ring, in mouse primordial oocytes. Live cell imaging of a mouse primordial oocyte, incubated with 3μM NBD C_6-Ceramide for 30 minutes to image Golgi Apparatus. Images of the oocyte were acquired at 10 second intervals for a total time of 3 minutes. The drift was corrected using the StackReg plugin in Fiji/ ImageJ. The movie is played at 5 frames/second. Scale bar: 5μm

Movie S 2. Mitochondria and Golgi ring of mouse primordial oocytes are spatially segregated. Live cell imaging of a mouse primordial oocyte, incubated with 3μM NBD C_6-Ceramide and 100nM MitoTracker Deep Red FM for 30 minutes to image Golgi Apparatus and mitochondria. Images of the oocyte were acquired at 30 second intervals for a total time of 5 minutes. The drift was corrected using the StackReg plugin in Fiji/ ImageJ. The movie is played at 1 frame/second. Scale bar: 5μm

Movie S3 to S6 Z-stacks of representative whole mount ovaries in Figure 4
Whole-mount immunostaining of neonatal ovaries with FOXO3A (magenta) and GM130 (green) antibodies. Movies S3 1hour untreated control, Movie S4 Brefeldin A(BFA) treated ovary, Movie S5 5 hours untreated control, Movie S6 4hour washed ovary after 1 hour BFA treatment.

MATERIALS AND METHODS

Ethics

Xenopus and mouse colonies used in this manuscript were housed in the Animal Facility of the Barcelona Biomedical Research Park (PRBB, Barcelona, Spain, EU). All animals were sacrificed by accredited animal facility personnel before extraction of their ovaries.

Ethical Committee permission to conduct the human oocytes aspect of this study was obtained from the Comité Étic d'Investigació Clínica CEIC-Parc de salut MAR (Barcelona) and Comité Ético de investigación Clínica CEIC-Hospital Clínic de Barcelona with approval number *HCB/2018/0497*. Written informed consent to participate was obtained from all participants prior to their inclusions in the study.

Animal Maintenance

Xenopus laevis fertile females were purchased from Nasco (NJ, USA). The C57BL/6J and CD1 mice used in the experiments were maintained in the Animal Facility of the Barcelona Biomedical Research Park (PRBB, Barcelona, Spain, EU) under specific pathogen-free conditions at 22°C with access to food and water ad libitum. Female mice with ages between 3 days and 7 weeks were used for experiments.

Primordial oocyte isolation

Mouse: Primordial oocytes from neonatal (Postnatal day 3 or 4) mice ovaries were isolated with a protocol modified from (Eppig and Wigglesworth, *Biol. Reprod*., 2000). Briefly, the ovaries were digested in 0.05% Trypsin-EDTA (Gibco, 25300-054) with 0.02% DNase I (Sigma, DN25-100mg) at 37ºC for 30 minutes. The resulting suspension was neutralized with an equal volume of medium M199 (Gibco, 41550-020) containing 10% FBS (Gibco, 26140-087), 2.5mM Na-Pyruvate (Thermo, 11360070), 0.2% Na-DL-Lactate syrup (Sigma, L7900), 1x Penicillin-Streptomycin (Gibco, 15070-063) and centrifuged at 850 rpm for 3 minutes. The supernatant was decanted, and cells were transferred to a petri dish (33 X 10 mm, Corning, 351008) and placed in an incubator at 37ºC and 5% CO_2. All mouse oocyte imaging experiments were conducted in the medium mentioned above.

Human Donations were provided by the gynecology service of Hospital Clinic Barcelona, from women aged 19 to 34 undergoing ovarian surgery. Donated ovarian cortex samples were transported in Leibovitz medium (Gibco, 21083-027) containing 3 mg/mL BSA (Heat Shock Fraction, Sigma A7906) and quickly cut into 3 mm cubic pieces. Ovary pieces were transferred to DMEM containing 25 mM HEPES (Gibco, 21063-029) and 2 mg/mL collagenase type III (Worthington Biochemical Corporation, LS004183) and were left for digestion in a 37°C incubator with a 5% CO2 atmosphere for 2 hours, with occasional swirling of the petri dishes (100 X 20 mm, Corning 353003). After 2 hours, the resulting suspension containing individual cells was separated from tissue fragments by sedimentation in a 50 mL falcon tube and collagenase III was neutralized adding a 1:1 amount of DMEM/F12 medium (Gibco, 11330-032) containing 15 mM HEPES and 10% FCS (Gibco, 10270106). Individual human follicles are several magnitudes larger in volume and thus heavier than other single cells in the suspension. Incorporating this feature of follicles into the isolation protocol vastly improved the efficiency of isolation: After transferring the above supernatant to petri dishes, oocytes sedimented to the bottom within 15 seconds. We then removed the top layers of the single cell suspension by suction to have a primordial follicle enriched petri dish, mostly cleaned from other cells of the ovary. Follicles were picked manually under a dissecting

microscope with a p10 pipette and transferred to a tissue culture dish. We obtain 60 to 180 primordial follicles from each of our ovary preparations. Leftover fragments of tissue were treated again for 2 hours with DMEM containing 25 mM HEPES and collagenase III for further 2 hours and follicles were picked as before. All human oocyte imaging experiments were conducted in the medium mentioned above.

Frog: Oocytes were isolated from young adult *Xenopus* (aged 3 to 5 years) ovaries according to the protocol described in (Boke et al., 2016). Briefly, ovaries were digested using 2mg/ml Collagenase IA (Sigma, C9891-1G) in MMR by gentle rocking until dissociated oocytes were visible, for 30 to 45 minutes. The resulting mix was passed through two sets of filter meshes, the first with 297 micron mesh size and the second with 250 micron mesh size (Spectra/Mesh, 146424, 146426). All washes were performed in MMR. Oocytes which passed through the 250 micron mesh were washed once more with MMR and transferred to OCM (Boke et al., 2016; Mir and Heasman, 2008). All frog oocyte imaging experiments were conducted in OCM at room temperature and atmospheric air.

Germinal vesicle oocyte isolation from mouse

Ovaries of 6-week-old mice were dissected in M2 medium (Sigma, M7167) to remove the fat pad and oviducts attached to the ovaries. The ovaries were punctured using an insulin needle to release germinal vesicle (GV) stage oocytes. The oocytes were collected with an oocyte manipulation pipette and transferred to a new dish containing M2 medium (Sigma, M7167) + 400μM dbcAMP (Sigma, D0627) and incubated at 37ºC, atmospheric air.

***In vitro* ovary culture**

Neonatal ovaries were dissected, cleaned of adjoining tissue in M2 medium (Sigma, M7167) and placed on Millicell hanging cell culture inserts (Merck, MCSP24H48) in a 24 well plate (Greiner bio-one, 662160). 500μL of DMEM/F12 medium (Gibco, 31331-028) supplemented with 10% FBS (Gibco, 26140-087) and 1x Penicillin-Streptomycin (Gibco, 15070-063) was introduced into each well such that a thin layer of liquid was present above the ovary. The ovaries were cultured for indicated times in an incubator at 37ºC and 5% CO_2.

Fluorescent Dyes

TMRE: Tetramethylrhodamine, Ethyl ester, Percholorate (TMRE) (Thermo, T669) was added to oocytes at a final concentration of 500nM and incubated for 30 minutes. Oocytes were washed and plated on 35mm glass bottom MatTek (MatTek Corporation, P35G-1.5-20-C) dishes in fresh medium.

Lysotracker: LysoTracker Deep Red (Thermo, L12492) was added to the oocytes at a final concentration of 50nM and incubated for 30 minutes. Oocytes were washed and plated on glass bottom MatTek dishes in fresh medium.

NBD C_6-Ceramide: Oocytes were incubated in medium containing NBD C_6-Ceramide (Thermo, N22651) to a final concentration of 3μM for 30 minutes at 37ºC and 5% CO_2. The oocytes were then washed and plated on MatTek dishes in fresh medium.

Proteostat: Staining was performed according to the manufacturer's instructions; 1:1000 final concentration of Proteostat was used.

Drug Treatments

CCCP treatment: Isolated oocytes were incubated in culture medium containing carbonyl cyanide m-chlorophenyl hydrazine (Abcam, ab141229) at a final concentration of 30μM for 15 minutes, followed by TMRE addition.

Bafilomycin A1 treatment: Isolated oocytes were incubated in a droplet of medium containing Bafilomycin A1 (Abcam, ab120497) at a final concentration of 100nM for 1 hour, followed by addition of LysoTracker Far Red.

Brefeldin A treatment: Isolated oocytes were incubated in culture media containing Brefeldin A (Abcam, ab120299) at a final concentration of 10μM for 1.5 hours. The Brefeldin A was washed and oocytes were incubated in medium containing NBD C_6-Ceramide. Whole P3 ovaries were placed on Millicell hanging cell culture inserts (Merck, MCSP24H48) in 500μL medium with 10μM Brefeldin A for 1 hour in a 24 well-plate (Greiner bio-one, 662160). The ovaries were then either fixed in 4% PFA and processed for whole-mount immunostaining or transferred for 4 hours to Brefeldin A free medium for 4 hours before fixing them.

Live-cell imaging

Mouse and human oocytes were imaged in their respective culture medium in a Leica TCS SP5 STED microscope using a 63x water immersion objective (N.A 1.20, Leica, 506279) with an incubation chamber maintained at 37ºC and 5% CO_2. Frog oocytes were imaged in OCM at room temperature and atmospheric air in a Leica TCS SP8 microscope using a 40x water immersion objective (N.A 1.10, Leica, 506357). All images were acquired using the Leica Application Suite X (LAS X) software. The images were analysed using Fiji/ ImageJ.

Immunostaining frozen ovary sections

Sample preparation – mouse: Neonatal (P3 or P4) ovaries were dissected in M2 medium (Sigma, M7167) to remove the surrounding tissue and fixed in 4% PFA in PBS at 4ºC for 3 hours. Ovaries were transferred to 30% Sucrose in PBS overnight at 4ºC. The next day, they were placed in OCT medium within a mould and sections of 10 or 20μM thickness were cut using a microtome and sections were transferred onto glass slides.
Sample preparation – human: Fragments of human ovary about 3mm x 3mm were taken from the cortex and fixed in 4% PFA in 100mM phosphate buffer pH 7.5 for 4 hours at room temperature. The fragments were then moved overnight to 30% Sucrose in PBS with shaking. Next day they were embedded in OCT medium in a mould. Sections of 10 or 20 μM thickness were cut using a microtome and transferred onto glass slides.
Immunostaining: Before carrying out immunostaining, the sections were equilibrated at room temperature for 10 minutes and washed in PBS for 15 minutes in coplin jars. The sections were then permeabilized (PBS containing 0.2% Triton X100 and 0.1% Tween-20) for 30 minutes and blocked using blocking buffer (PBS containing 3% BSA and 0.05% Tween-20) for 1 hour. Using a hydrophobic pen, boxes were drawn around the sections. The primary antibodies were against GM130 (1:100, BD, 610822), TGN46 (1:100, Abcam, ab16059), Pericentrin (1:100, Abcam, ab4448), RNGTT(1:100, ab201046) and Citrate Synthase (1:100, ab96600). The primary antibodies were diluted in 200μL blocking solution, added to the sections and incubated overnight at 4ºC. The next day, sections were washed in PBS for 15 minutes. Secondary antibodies goat anti-mouse Alexa488 (1:1000, Invitrogen, A32723) and goat anti-rabbit Alexa647 (1:1000, Invitrogen, A21245) were diluted in 200μL blocking solution and added to the sections

and incubated for 2 hours in the dark at room temperature. The sections were washed for 30 minutes in PBS and briefly rinsed with water. A droplet of mounting medium containing DAPI (Abcam, ab104139) was added onto the section and a coverslip was carefully placed on top. The coverslip was then sealed on the edges with nail polish and allowed to dry in the dark. Imaging was carried out in Leica TCS SP5 or Leica TCS SP8 microscopes using 63x oil immersion objectives (N.A 1.40, Leica 15506350). The images were analyzed using Fiji/ ImageJ.

Immunostaining GV oocytes

GV oocytes were isolated as described above and fixed for 30 minutes in 4% PFA in 100mM phosphate buffer, pH 7.4. The oocytes were washed in PBS by transferring them using a oocyte manipulation pipette and blocked with Blocking buffer containing 3% BSA in PBS with 0.1% Triton X-100. The oocytes were incubated in primary antibody RAP55b (1:100, Abcam, ab221041) diluted in blocking buffer, overnight at 4ºC. The next day, they were washed in blocking buffer and incubated with secondary antibody goat anti-rabbit Alexa647 (1:500, Invitrogen, A21245) diluted in blocking buffer for 1 hour at room temperature. The oocytes were then washed overnight in blocking buffer at 4ºC, placed on glass bottom MatTek dishes in 10μl droplets of PBS and covered with oil (Sigma, M8410) Imaging was carried out in Leica TCS SP5 or Leica TCS SP8 microscopes using 63x oil immersion objectives (N.A 1.40, Leica, 11506350). The images were analyzed using Fiji/ ImageJ.

Whole-mount immunostaining

The protocol for whole-mount immunostaining was modified from the protocol described by (Rinaldi et al., 2018). Briefly, ovaries were fixed in 4% PFA at 4°C, 3 hours, transferred to PBS or 70% Ethanol and incubated overnight. The tissue was permeabilized and blocked according to the protocol. The ovaries were then incubated with primary antibodies (rabbit anti-FOXO3a [Cell Signal, 2497S] and mouse anti-GM130 in case of ovaries transferred to PBS after fixation; rabbit anti-LSM14b, rabbit LSM14a [Thermo, PA5-78464] and mouse anti-DDX4 [Abcam, ab27591], or mouse anti-DDX6 [SCBT, sc-376433] in case of ovaries transferred to 70% Ethanol after fixation) in the ratio of 1:100 for each antibody in blocking solution for 48 hours. After washing the ovaries overnight in wash buffer, they were incubated with 1:1000 of secondary antibodies goat anti-mouse Alexa488 (1:1000, Invitrogen, A32723) and goat anti-rabbit Alexa647 (1:1000, Invitrogen, A21245) in blocking solution for 48 hours. The ovaries were washed overnight with wash buffer and next day, replaced with DAPI at a final concentration of 50μg/ml in wash buffer for 8 hours and washed overnight in fresh wash buffer. The ovaries were imaged in a droplet of PBS on a MatTek dish using a Leica TCS SP8 microscope with 20x air (N.A 0.70, Leica, 11506166) or 40x oil immersion (11506358, Leica, N.A 1.30) objective. The images were analysed using Fiji/ ImageJ.

FOXO3a localization and GM130 ring quantification

Z-stacks of 20μm were made by imaging whole-mount ovaries at 1μm sections. The oocytes were marked by creating ROIs in Fiji ROI Manager based on FOXO3a, GM130 and DAPI staining. FOXO3a staining was assessed manually as nuclear, cytoplasmic or nucleo-cytoplasmic and the number of oocytes in each case was recorded. Similarly, the presence of the Golgi ring as seen by GM130 staining was counted in these oocytes. Nuclear FOXO3a and the presence of the Golgi ring were quantified for ovaries cultured *in vitro* for 0, 1 and 5 hours in the absence of BFA (untreated), treated with BFA for 1 hour and treated with BFA for 1 hour followed by a 4-hour washout. The corresponding values at each time point were plotted by JMP Statistical Software.

Mitochondrial occupancy calculation

Oocytes isolated from neonatal (P3 or P4) mice were treated with Brefeldin A, stained with 3μM NBD C_6-ceramide and 100nM MitoTracker Deep Red FM (Thermo, M22426) to visualize the Golgi Apparatus and mitochondria. After 30 minutes, the oocytes were washed, plated on MatTek dishes and imaged live. The area of the oocyte cytoplasm was determined by subtracting the area of the nucleus from the whole area of the oocytes (Figure S3). A mask was created to select mitochondria using the threshold function in Fiji/ Image J. The mitochondrial occupancy was then calculated as

$$Mitochondrial\ occupancy\ (\%) = \frac{area\ occupied\ by\ mitochondria}{area\ of\ oocyte\ cytoplasm} \times\ 100$$

Significance of the difference in mitochondrial occupancy in untreated versus BFA treated oocytes was assessed using student's t test.

ACKNOWLEDGEMENTS

We would like to thank PRBB Animal Facility personnel for their continued support. We are grateful to Histology Facility (Alexis Rafols Mitjans) and the Advanced Light Microscopy team (especially Timo Zimmerman) for their support. This study was supported by an ERC Starting Grant (ERC-StG-2017-759107), and a Ministerio de Economía y Competitividad Grant (MINECO - BFU2017-89373-P) to Elvan Böke.

The authors declare no competing financial interests.

AUTHOR CONTRIBUTIONS

E.B. conceived and designed the project, performed *Xenopus* experiments and helped perform human oocyte isolation and imaging experiments with J.M.D. All mouse experiments were performed by L.D except for Fig6D (J.M.D). M.S helped devising oocyte isolation protocols and ovary isolations. C.D.G and M.A.M.Z informed patients and supervised the collection of human ovarian cortex from surgeries. The manuscript was written by L.D. and E.B. with input from all authors.

REFERENCES

Al-Mukhtar, K.A., and A.C. Webb. 1971. An ultrastructural study of primordial germ cells, oogonia and early oocytes in Xenopus laevis. *Development*. 26:195-217.

Amselgruber, V.W. 1983. Licht-und elektronenmikroskopische Untersuchungen zur Oogenese der Katze (Felis catus). *Anatomia, Histologia, Embryologia*. 12:193-229.

Avidor-Reiss, T., and E.L. Fishman. 2019. It takes two (centrioles) to tango. *Reproduction*. 157:R33-R51.

Baca, M., and L. Zamboni. 1967. The fine structure of human follicular oocytes. *Journal of ultrastructure research*. 19:354-381.

Bilinski, S.M., M. Kloc, and W. Tworzydlo. 2017. Selection of mitochondria in female germline cells: is Balbiani body implicated in this process? *Journal of assisted reproduction and genetics*. 34:1405-1412.

Bisel, B., Y. Wang, J.-H. Wei, Y. Xiang, D. Tang, M. Miron-Mendoza, S.-i. Yoshimura, N. Nakamura, and J. Seemann. 2008. ERK regulates Golgi and centrosome orientation towards the leading edge through GRASP65. *The Journal of cell biology*. 182:837-843.

Bohnert, K.A., and C. Kenyon. 2017. A lysosomal switch triggers proteostasis renewal in the immortal C. elegans germ lineage. *Nature*. 551:629-633.

Boke, E., M. Ruer, M. Wühr, M. Coughlin, R. Lemaitre, S.P. Gygi, S. Alberti, D. Drechsel, A.A. Hyman, and T.J. Mitchison. 2016. Amyloid-like self-assembly of a cellular compartment. *Cell*. 166:637-650.

Bowman, E.J., A. Siebers, and K. Altendorf. 1988. Bafilomycins: a class of inhibitors of membrane ATPases from microorganisms, animal cells, and plant cells. *Proceedings of the National Academy of Sciences*. 85:7972-7976.

Callen, J., N. Dennebouy, and J. Mounolou. 1980. Kinetic analysis of entire oogenesis in Xenopus laevis. *Development, Growth & Differentiation*. 22:831-840.

Castrillon, D.H., L. Miao, R. Kollipara, J.W. Horner, and R.A. DePinho. 2003. Suppression of ovarian follicle activation in mice by the transcription factor Foxo3a. *Science*. 301:215-218.

Clift, D., and M. Schuh. 2013. Restarting life: fertilization and the transition from meiosis to mitosis. *Nature reviews Molecular cell biology*. 14:549-562.

Cox, R.T., and A.C. Spradling. 2003. A Balbiani body and the fusome mediate mitochondrial inheritance during Drosophila oogenesis. *Development*. 130:1579-1590.

Doxsey, S.J., P. Stein, L. Evans, P.D. Calarco, and M. Kirschner. 1994. Pericentrin, a highly conserved centrosome protein involved in microtubule organization. *Cell*. 76:639-650.

Ehrenberg, B., V. Montana, M. Wei, J. Wuskell, and L. Loew. 1988. Membrane potential can be determined in individual cells from the nernstian distribution of cationic dyes. *Biophysical journal*. 53:785-794.

Eppig, J.J. 2001. Oocyte control of ovarian follicular development and function in mammals. *Reproduction*. 122:829-838.

Flurkey, K., J.M. Currer, and D. Harrison. 2007. Mouse models in aging research. *In* The mouse in biomedical research. Elsevier. 637-672.

Galloway, A., and V.H. Cowling. 2019. mRNA cap regulation in mammalian cell function and fate. *Biochimica et Biophysica Acta (BBA)-Gene Regulatory Mechanisms*. 1862:270-279.

Grive, K.J., and R.N. Freiman. 2015. The developmental origins of the mammalian ovarian reserve. *Development*. 142:2554-2563.

Guo, J., T. Zhang, Y. Guo, T. Sun, H. Li, X. Zhang, H. Yin, G. Cao, Y. Yin, and H. Wang. 2018. Oocyte stage-specific effects of MTOR determine granulosa cell fate and oocyte quality in mice. *Proceedings of the National Academy of Sciences*. 115:E5326-E5333.

Handel, M.A., J.J. Eppig, and J.C. Schimenti. 2014. Applying “gold standards” to in-vitro-derived germ cells. *Cell*. 157:1257-1261.

Hayashi, K., S. Shimamoto, and G. Nagamatsu. 2020. Environmental factors for establishment of the dormant state in oocytes. *Development, Growth & Differentiation*. 62:150-157.

Hertig, A.T. 1968. The primary human oocyte: some observations on the fine structure of Balbiani's vitelline body and the origin of the annulate lamellae. *Developmental Dynamics*. 122:107-137.

Hertig, A.T., and E.C. Adams. 1967. Studies on the human oocyte and its follicle. *The Journal of Cell Biology*. 34:647-675.

Heytler, P. 1963. Uncoupling of oxidative phosphorylation by carbonyl cyanide phenylhydrazones. I. Some characteristics of m-Cl-CCP action on mitochondria and chloroplasts. *Biochemistry*. 2:357-361.

Holubcová, Z., M. Blayney, K. Elder, and M. Schuh. 2015. Error-prone chromosome-mediated spindle assembly favors chromosome segregation defects in human oocytes. *Science*. 348:1143-1147.

Hope, J. 1965. The fine structure of the developing follicle of the rhesus ovary. *Journal of ultrastructure research*. 12:592-610.

Huch, S., J. Gommlich, M. Muppavarapu, C. Beckham, and T. Nissan. 2016. Membrane-association of mRNA decapping factors is independent of stress in budding yeast. *Scientific reports*. 6:1-16.

Jamieson-Lucy, A., and M.C. Mullins. 2019. The vertebrate Balbiani body, germ plasm, and oocyte polarity. *In* Current topics in developmental biology. Vol. 135. Elsevier. 1-34.

Keem, K., L.D. Smith, R.A. Wallace, and D. Wolf. 1979. Growth rate of oocytes in laboratory-maintained Xenopus laevis. *Gamete Research*. 2:125-135.

Kilchert, C., J. Weidner, C. Prescianotto-Baschong, and A. Spang. 2010. Defects in the secretory pathway and high Ca2+ induce multiple P-bodies. *Molecular biology of the cell*. 21:2624-2638.

Kloc, M., S. Bilinski, and L.D. Etkin. 2004. The Balbiani body and germ cell determinants: 150 years later. *In* Current topics in developmental biology. Vol. 59. Elsevier. 1-36.

Koga, D., and T. Ushiki. 2006. Three-dimensional ultrastructure of the Golgi apparatus in different cells: high-resolution scanning electron microscopy of osmium-macerated tissues. *Archives of histology and cytology*. 69:357-374.

Kreft, M.E., D. Di Giandomenico, G.V. Beznoussenko, N. Resnik, A.A. Mironov, and K. Jezernik. 2010. Golgi apparatus fragmentation as a mechanism responsible for uniform delivery of uroplakins to the apical plasma membrane of uroepithelial cells. *Biology of the Cell*. 102:593-607.

Krishnakumar, P., S. Riemer, R. Perera, T. Lingner, A. Goloborodko, H. Khalifa, F. Bontems, F. Kaufholz, M.A. El-Brolosy, and R. Dosch. 2018. Functional equivalence of germ plasm organizers. *PLoS genetics*. 14:e1007696.

Lei, L., K. Ikami, H. Abbott, and S. Jin. 2020. The mouse Balbiani body maintains primordial follicle quiescence via RNA storage. *bioRxiv*.

Lei, L., and A.C. Spradling. 2016. Mouse oocytes differentiate through organelle enrichment from sister cyst germ cells. *Science*. 352:95-99.

Lippincott-Schwartz, J., J.G. Donaldson, A. Schweizer, E.G. Berger, H.-P. Hauri, L.C. Yuan, and R.D. Klausner. 1990. Microtubule-dependent retrograde transport of proteins into the ER in the presence of brefeldin A suggests an ER recycling pathway. *Cell*. 60:821-836.

Lipsky, N.G., and R.E. Pagano. 1985. A vital stain for the Golgi apparatus. *Science*. 228:745-747.

Lu, Z., D. Joseph, E. Bugnard, K.J. Zaal, and E. Ralston. 2001. Golgi complex reorganization during muscle differentiation: visualization in living cells and mechanism. *Molecular Biology of the Cell*. 12:795-808.

Marlow, F.L. 2017. Mitochondrial matters: mitochondrial bottlenecks, self-assembling structures, and entrapment in the female germline. *Stem cell research*. 21:178-186.

Marlow, F.L., and M.C. Mullins. 2008. Bucky ball functions in Balbiani body assembly and animal–vegetal polarity in the oocyte and follicle cell layer in zebrafish. *Developmental biology*. 321:40-50.

Matzuk, M.M., K.H. Burns, M.M. Viveiros, and J.J. Eppig. 2002. Intercellular communication in the mammalian ovary: oocytes carry the conversation. *Science*. 296:2178-2180.

Mir, A., and J. Heasman. 2008. How the mother can help: studying maternal Wnt signaling by anti-sense-mediated depletion of maternal mRNAs and the host transfer technique. *In* Wnt Signaling. Springer. 417-429.

Nelson, R., M.R. Sawaya, M. Balbirnie, A.Ø. Madsen, C. Riekel, R. Grothe, and D. Eisenberg. 2005. Structure of the cross-β spine of amyloid-like fibrils. *Nature*. 435:773-778.

Olzscha, H., O. Fedorov, B.M. Kessler, S. Knapp, and N.B. La Thangue. 2017. CBP/p300 bromodomains regulate amyloid-like protein aggregation upon aberrant lysine acetylation. *Cell chemical biology*. 24:9-23.

Pagano, R.E., M.A. Sepanski, and O.C. Martin. 1989. Molecular trapping of a fluorescent ceramide analogue at the Golgi apparatus of fixed cells: interaction with endogenous lipids provides a trans-Golgi marker for both light and electron microscopy. *The Journal of Cell Biology*. 109:2067-2079.

Pan, H., M.J. O'Brien, K. Wigglesworth, J.J. Eppig, and R.M. Schultz. 2005. Transcript profiling during mouse oocyte development and the effect of gonadotropin priming and development in vitro. *Developmental biology*. 286:493-506.

Pepling, M.E., J.E. Wilhelm, A.L. O'Hara, G.W. Gephardt, and A.C. Spradling. 2007. Mouse oocytes within germ cell cysts and primordial follicles contain a Balbiani body. *Proceedings of the National Academy of Sciences*. 104:187-192.

Pfender, S., V. Kuznetsov, M. Pasternak, T. Tischer, B. Santhanam, and M. Schuh. 2015. Live imaging RNAi screen reveals genes essential for meiosis in mammalian oocytes. *Nature*. 524:239-242.

Rao, S., G.W. Kirschen, J. Szczurkowska, A. Di Antonio, J. Wang, S. Ge, and M. Shelly. 2018. Repositioning of somatic golgi apparatus is essential for the dendritic establishment of adult-born hippocampal neurons. *Journal of Neuroscience*. 38:631-647.

Reddy, P., W. Zheng, and K. Liu. 2010. Mechanisms maintaining the dormancy and survival of mammalian primordial follicles. *Trends in Endocrinology & Metabolism*. 21:96-103.

Rimon-Dahari, N., L. Yerushalmi-Heinemann, L. Alyagor, and N. Dekel. 2016. Ovarian folliculogenesis. *In* Molecular mechanisms of cell differentiation in gonad development. Springer. 167-190.

Rinaldi, V.D., J.C. Bloom, and J.C. Schimenti. 2018. Whole mount immunofluorescence and follicle quantification of cultured mouse ovaries. *JoVE (Journal of Visualized Experiments)*:e57593.

Rugh, R. 1968. The mouse; its reproduction and development. Burgess Pub. Co.

Shimamoto, S., Y. Nishimura, G. Nagamatsu, N. Hamada, H. Kita, O. Hikabe, N. Hamazaki, and K. Hayashi. 2019. Hypoxia induces the dormant state in oocytes through expression of Foxo3. *Proceedings of the National Academy of Sciences*. 116:12321-12326.

Sieber, M.H., M.B. Thomsen, and A.C. Spradling. 2016. Electron transport chain remodeling by GSK3 during oogenesis connects nutrient state to reproduction. *Cell*. 164:420-432.

Sütterlin, C., and A. Colanzi. 2010. The Golgi and the centrosome: building a functional partnership. *Journal of Cell Biology*. 188:621-628.

Tao, C.-C., K.-M. Cheng, Y.-L. Ma, W.-L. Hsu, Y.-C. Chen, J.-L. Fuh, W.-J. Lee, C.-C. Chao, and E.H. Lee. 2020. Galectin-3 promotes Aβ oligomerization and Aβ toxicity in a mouse model of Alzheimer's disease. *Cell Death & Differentiation*. 27:192-209.

Usmani, S.M., O. Zirafi, J.A. Müller, N.L. Sandi-Monroy, J.K. Yadav, C. Meier, T. Weil, N.R. Roan, W.C. Greene, and P. Walther. 2014. Direct visualization of HIV-enhancing endogenous amyloid fibrils in human semen. *Nature communications*. 5:1-8.

Wallace, W.H.B., and T.W. Kelsey. 2010. Human ovarian reserve from conception to the menopause. *PloS one*. 5:e8772.

Watanabe, T., Y. Sakai, D. Koga, H. Bochimoto, Y. Hira, M. Hosaka, and T. Ushiki. 2012. A unique ball-shaped Golgi apparatus in the rat pituitary gonadotrope: its functional implications in relation to the arrangement of the microtubule network. *Journal of Histochemistry & Cytochemistry*. 60:588-602.

Wilhelm, J.E., M. Buszczak, and S. Sayles. 2005. Efficient protein trafficking requires trailer hitch, a component of a ribonucleoprotein complex localized to the ER in Drosophila. *Developmental cell*. 9:675-685.

Wischnitzer, S. 1970. An electron microscope study of cytoplasmic organelle transformations in developing mouse oocytes. *Wilhelm Roux'Archiv für Entwicklungsmechanik der Organismen*. 166:150-172.

Zhang, Y.-Z. 1994. Novel fluorescent acidic organelle-selective dyes and mitochondrion-selective dyes that are well retained during cell fixation and permeabilization. *Mol. Biol. Cell*. 5:113a.

Figure 1

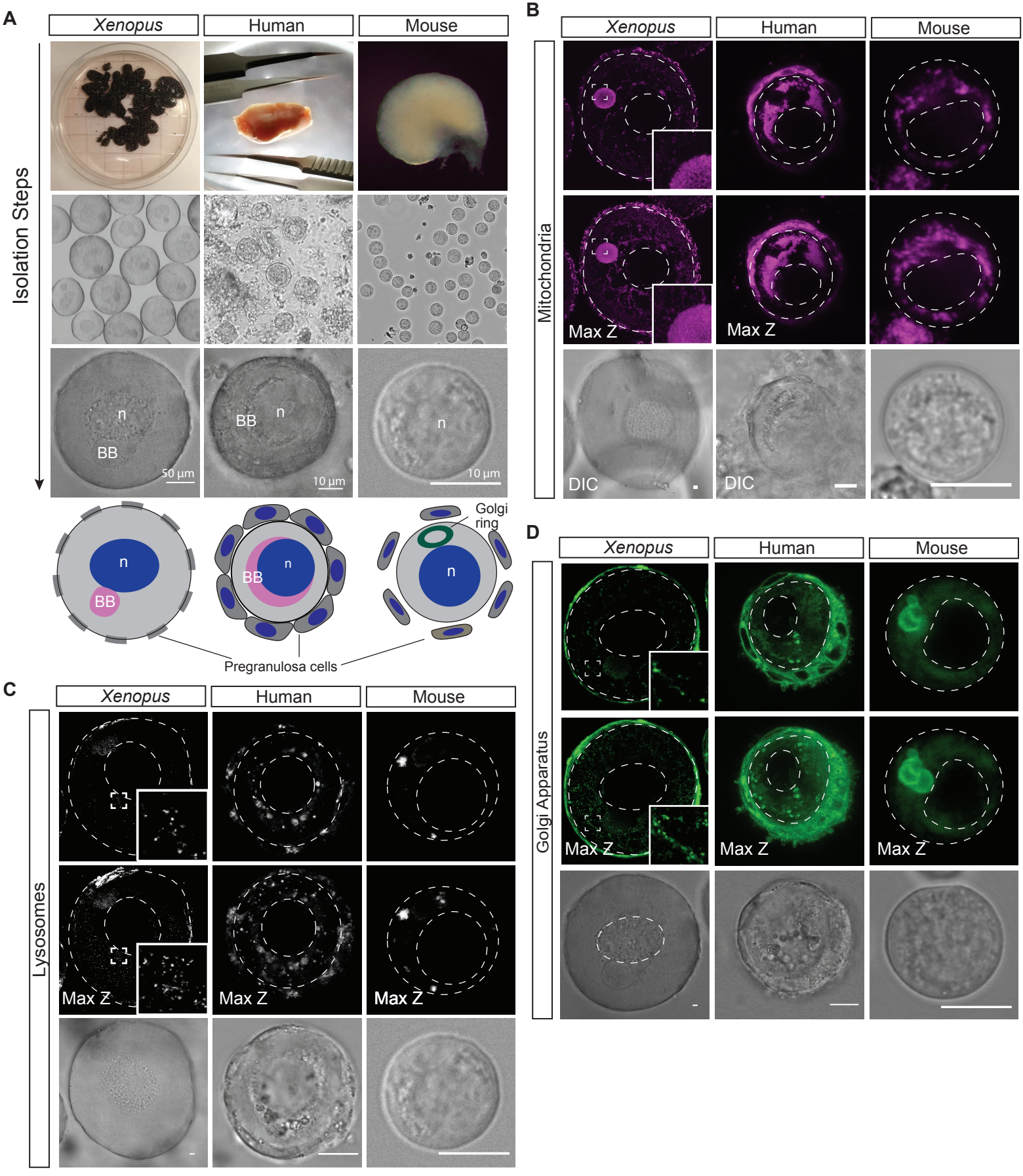
A
Xenopus
Human
Mouse
Isolation Steps
n
BB
50 µm
10 µm
Golgi ring
Pregranulosa cells
B
Mitochondria
Max Z
DIC
C
Lysosomes
D
Golgi Apparatus

Figure 2

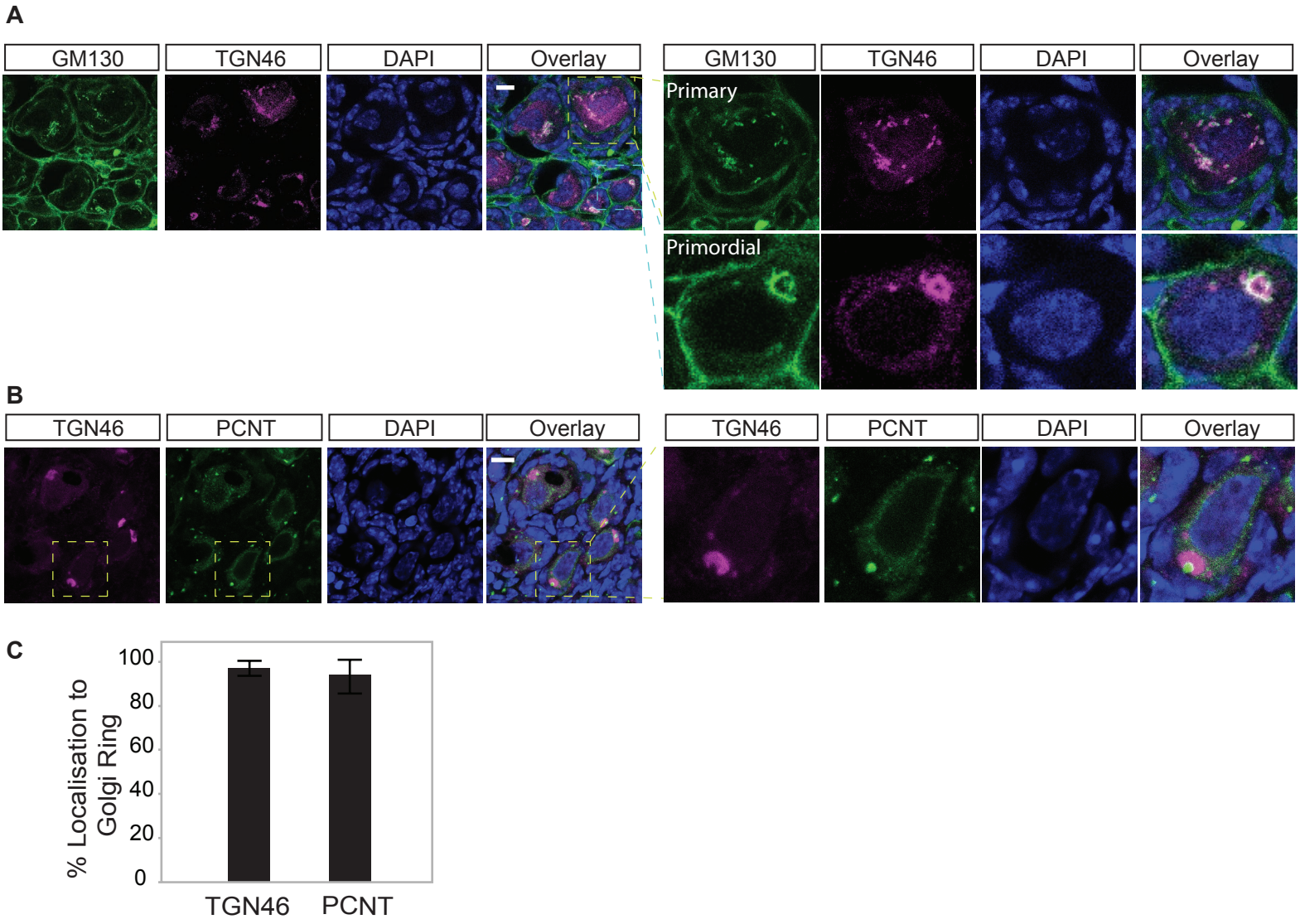

Figure 3

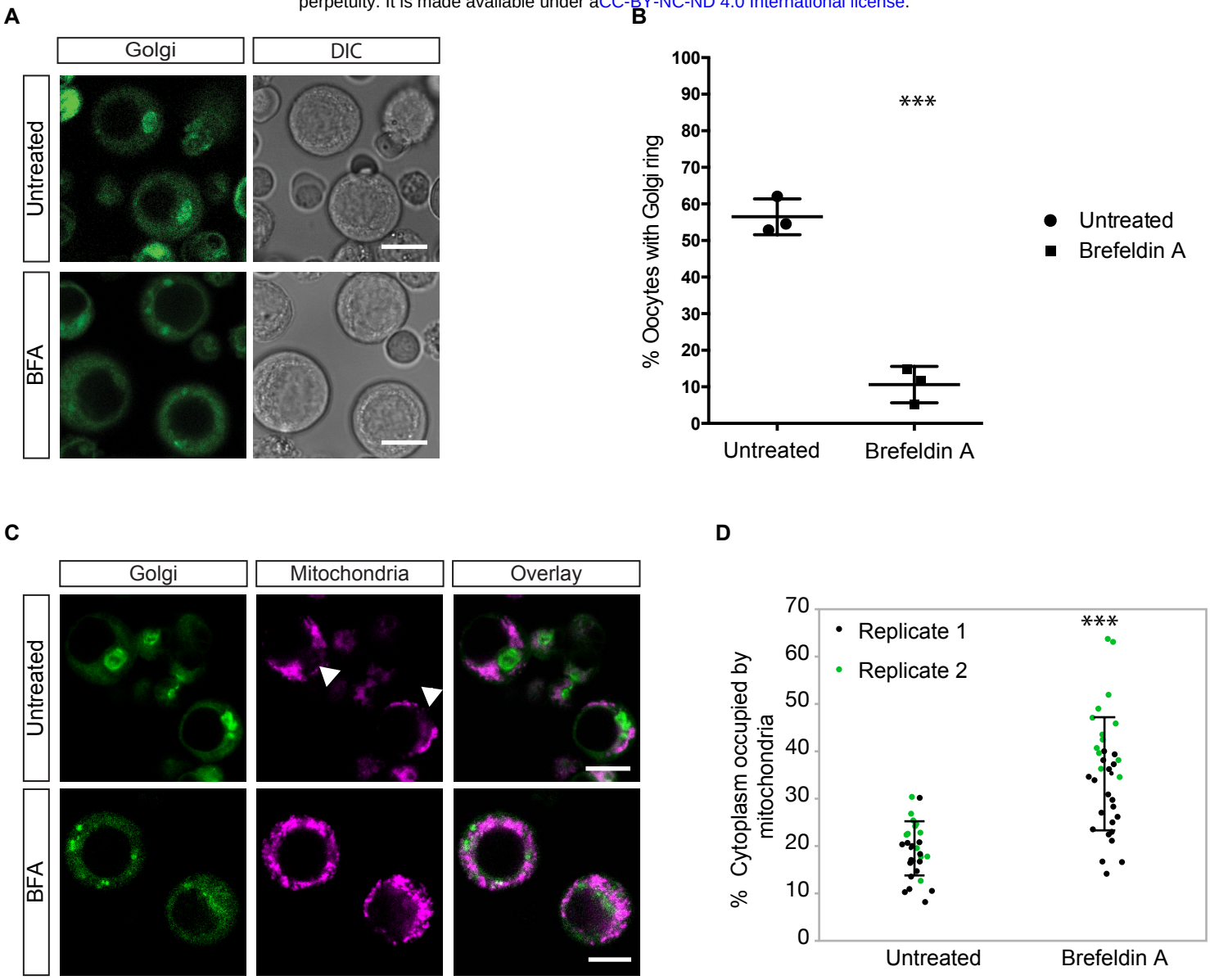

Figure 4

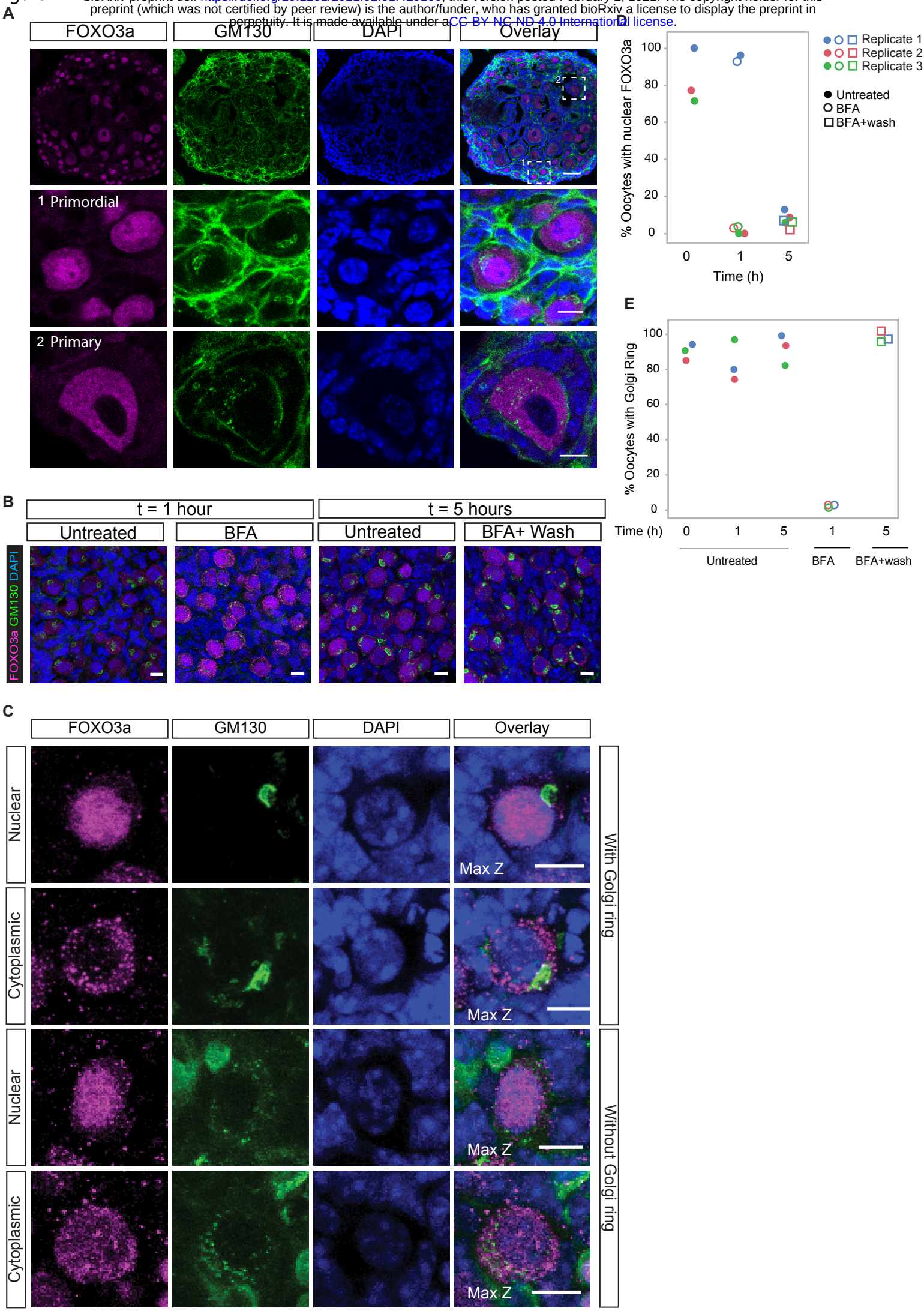

Figure 5

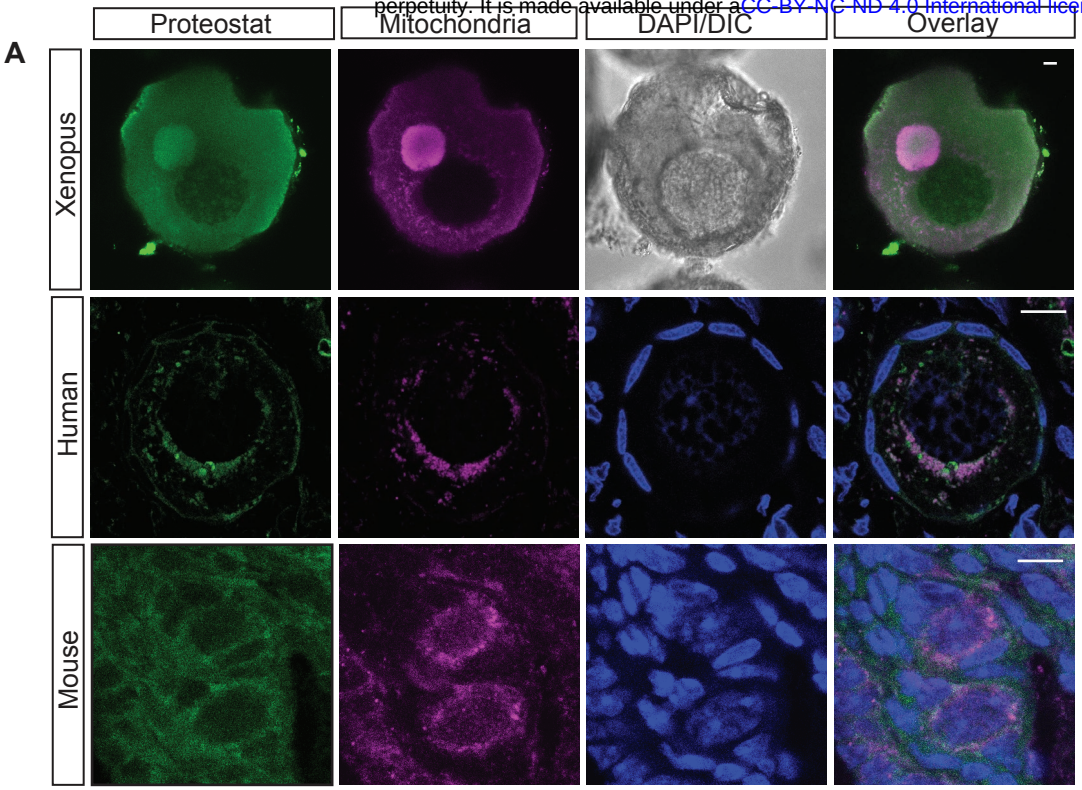

Supplementary Figure 1

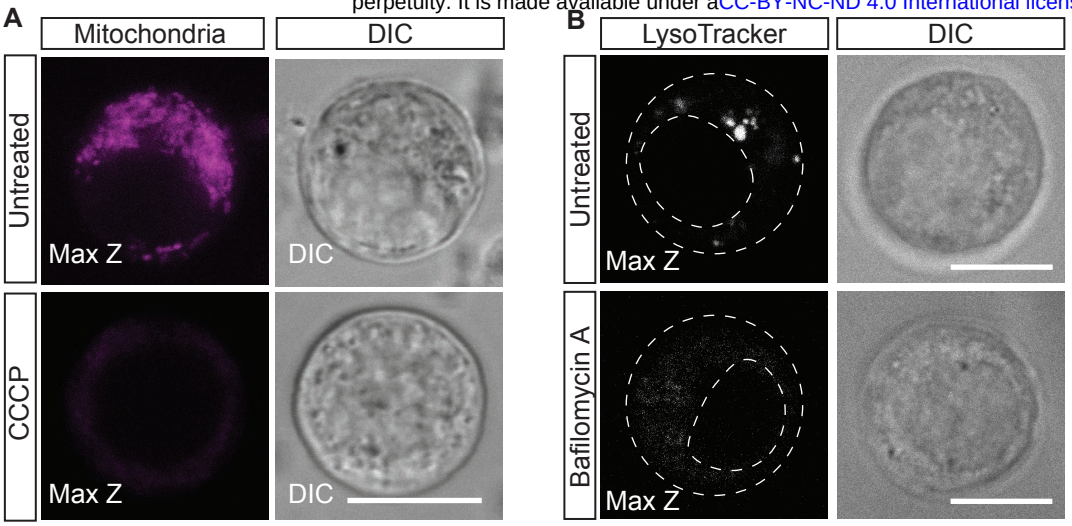

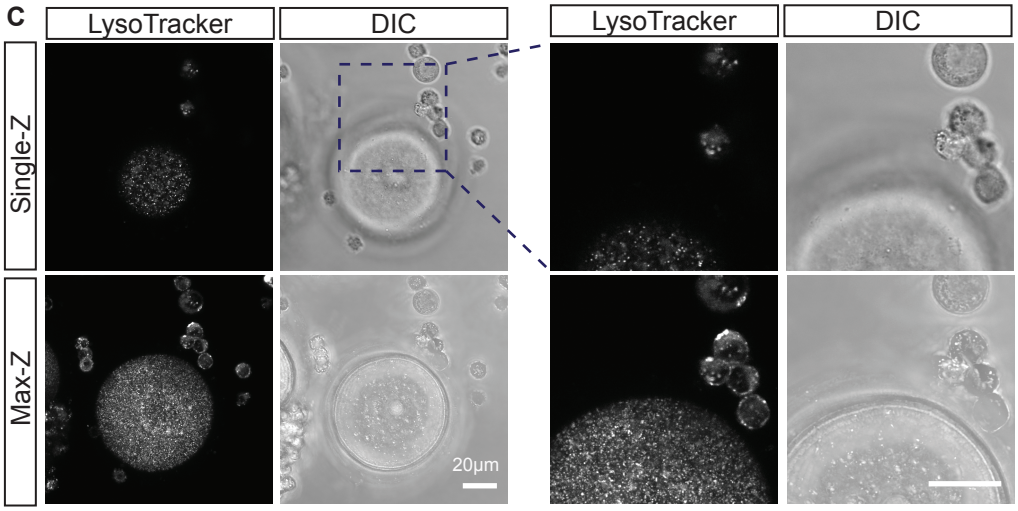

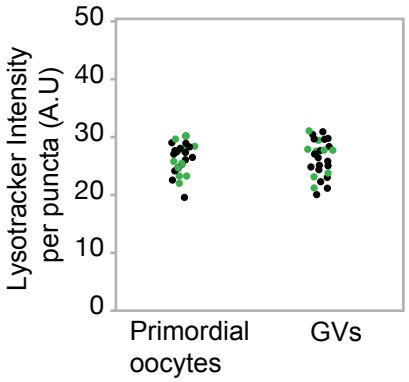

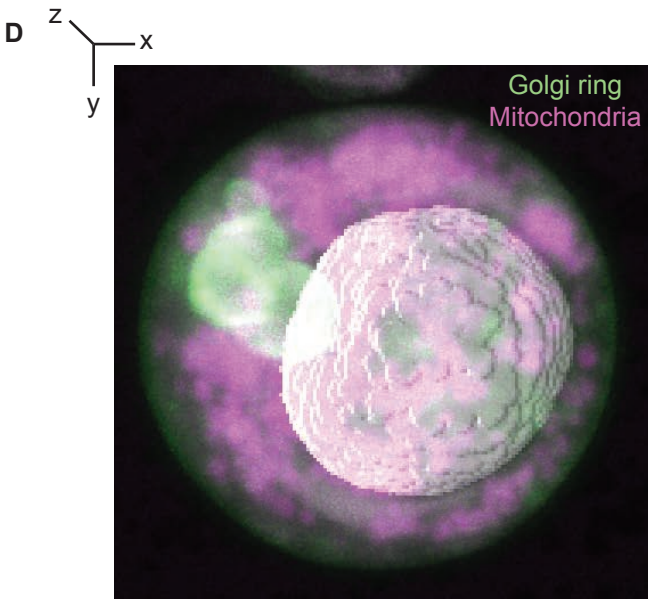

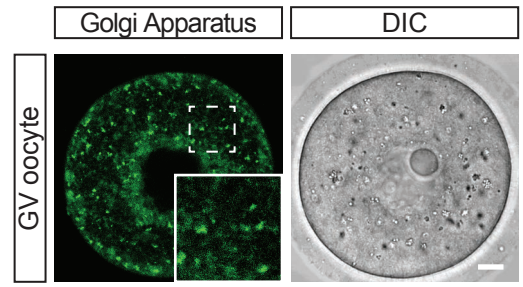

Supplementary Figure 2

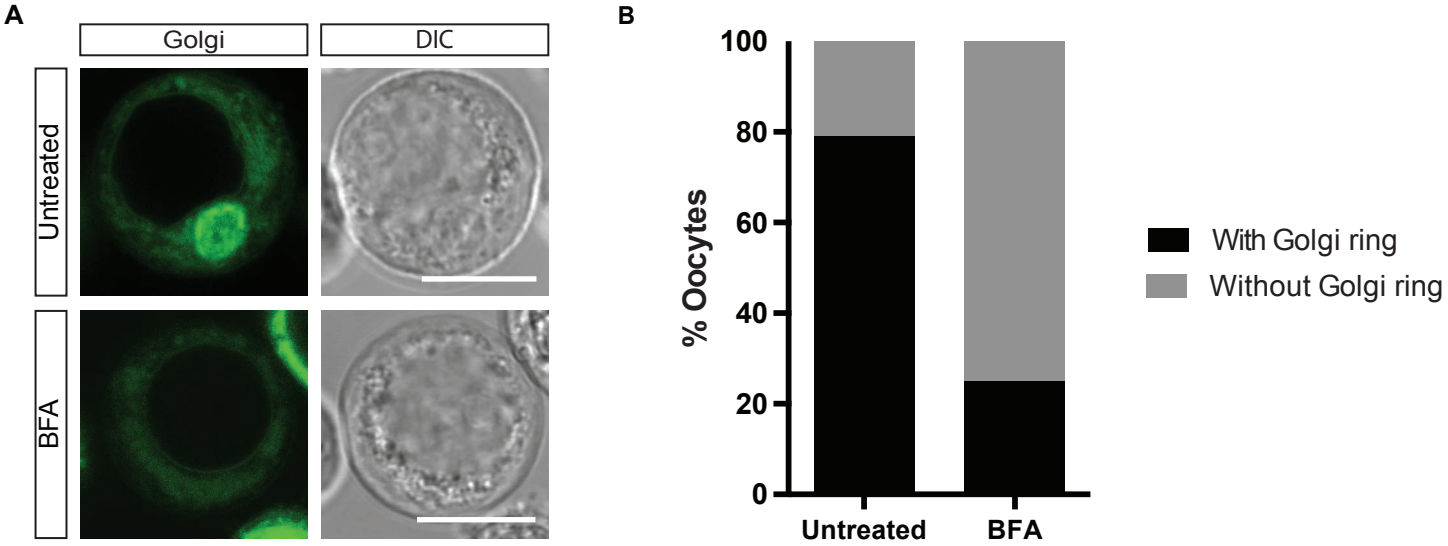

Supplementary Figure 3

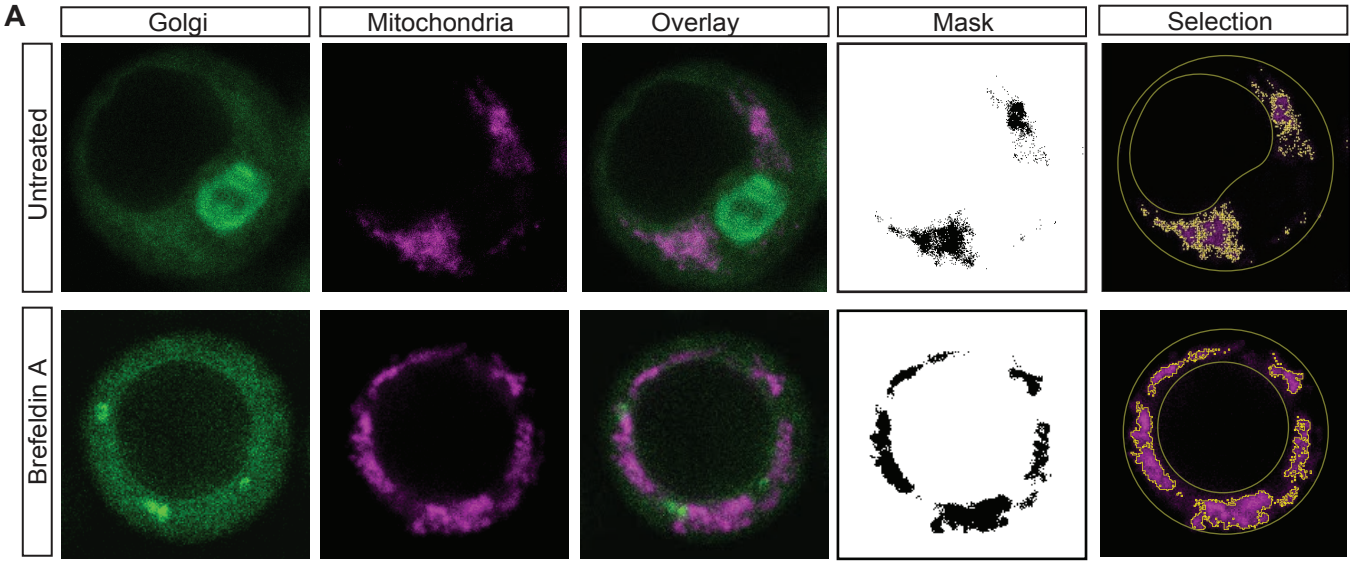

Supplementary Figure 4

A

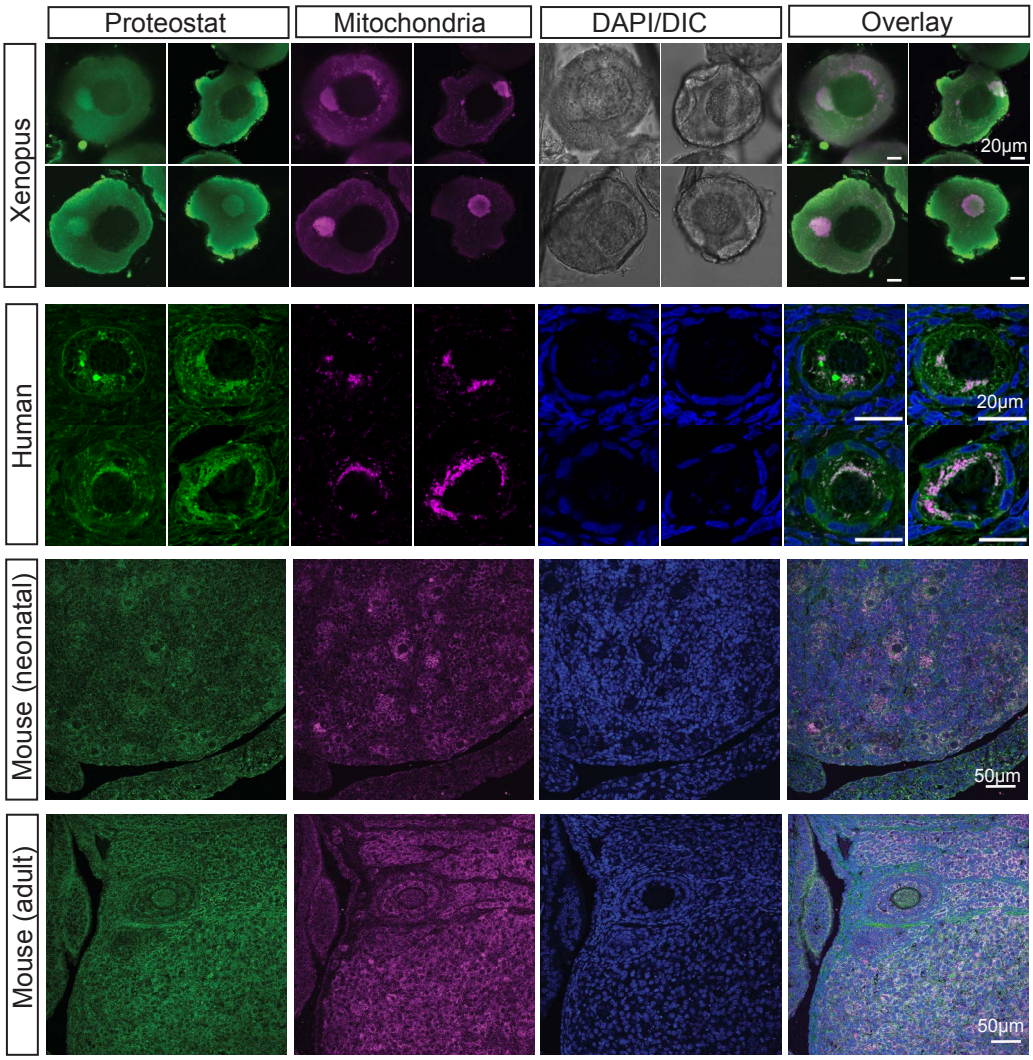

Supplementary Figure 5